Heat Mass Transfer
DOI 10.1007/s00231-015-1564-9

ORIGINAL

Efficiency analysis of organic Rankine cycle with internal heat exchanger using neural network

Fatih Yılmaz[1] · Reşat Selbaş[1] · Arzu Şencan Şahin[1]

Received: 22 April 2014 / Accepted: 4 April 2015

Abstract In this study, artificial neural network (ANN) has been used for efficiency analysis of the organic Rankine cycle with internal heat exchanger (IHEORC) using refrigerants R410a, R407c which do not damage to ozone layer. It is well known that the evaporator temperature, condenser temperature, subcooling temperature and superheating temperature affect the thermal efficiency of IHEORC. In this study, thermal efficiency is estimated depending on the above temperatures. The results of ANN are compared with actual results. The coefficient of determination values obtained when the test set were used to the networks were 0.99946 and 0.999943 for the R410a and R407c respectively which is very satisfactory.

1 Introduction

The interest for low grade heat recovery has been growing for the last 10 years, due to the increasing concern over energy shortage and global warming. An important number of new solutions have been proposed to generate electricity from low temperature heat sources. Among the proposed solutions, the organic Rankine cycle (ORC) system is the most widely used [1, 2]. An ORC system is similar to a conventional steam cycle energy conversion system. However, for such a system, the working fluid is an organic fluid such as refrigerants and hydrocarbons characterized by a lower boiling temperature. Figure 1 shows ORC with internal heat exchanger. It consists of an evaporator driven by the geothermal source (or waste heat source), a turbine, an internal heat exchanger, a condenser, and a pump.

In recent years, studies in the literature on ORC systems have been increased. Tchanche et al. [1] presented a review of ORC applications. These applications include solar thermal electricity, solar thermal driven reverse osmosis desalination, Duplex-Rankine cooling, solar pond power systems, ocean thermal energy conversion, biomass combined heat and power plants, binary geothermal systems and low-grade waste heat recycling from thermal devices and processes.

Algieri and Morrone [2] investigated the energetic performance of subcritical and transcritical ORCs. The influence of the operating conditions on system performances has been evaluated. Cyclohexane, decane and toluene have been used as working fluids. The biomass energy was used for the ORC. Chen et al. [3] presented a design method for the thermodynamic analysis for ORCs. The results show that a higher turbine inlet temperature requires a lower turbine inlet pressure, leading to a lower system thermal efficiency. The maximum thermal efficiency appears at the saturated or slightly-superheated vapor state at the turbine inlet. The pinch temperature differences in evaporators strongly influence the system thermal efficiency. Delgado-Torres and Garcia-Rodriguez [4] carried out analysis and optimization of the low-temperature solar ORC. Twelve substances are considered as working fluids of the ORC and four different models of stationary solar collectors. Results obtained for the solar regenerative ORC show that, in general, dry fluids considered yield lower values of the unit aperture area than wet fluids with the exception of ammonia. Ammonia yields similar values than isobutene

✉ Arzu Şencan Şahin
sencan@tef.sdu.edu.tr; arzusencan@sdu.edu.tr

Fatih Yılmaz
yilmaz_07@hotmail.com

Reşat Selbaş
resatselbas@sdu.edu.tr

[1] Technology Faculty, Süleyman Demirel University, 32260 Isparta, Turkey

Published online: 14 April 2015

and it has very good transport properties. However, it has higher values of saturation pressure and toxicity levels than the rest of the fluids considered in this work.

Kuo et al. [5] analyzed the system performance of a 50 kW ORC system subjected to influence of various working fluids. The thermal efficiency of an ORC system is strongly related to thermophysical properties. Analysis of the typical ORC heat exchangers indicates that the dominant thermal resistance in the shell-and-tube condenser is on the shell side. Kang [6] designed an ORC that generates electric power and uses R245fa as the working fluid. The performance of the developed cycle was investigated experimentally. The efficiencies of the cycle and the turbine, electric power of the developed ORC with respect to the operation conditions were investigated.

Aljundi [7] analyzed the effect of using alternative dry fluids on the efficiencies of the ORC. The effect of the critical temperature on the thermal and exergetic efficiencies was determined. It was found that efficiencies correlate with the critical temperature of the working fluid. Wang et al. [8] presented fluid selection and parametric optimization of ORC using low temperature waste heat. The effect of waste heat temperature and pinch point on the performance and economic characteristics of ORC system was compared under the optimal conditions.

Sun and Li [9] presented a detailed analysis of an ORC heat recovery power plant using R134a as working fluid. Mathematical models for expander, evaporator, and air cooled condenser and pump are developed to evaluate the plant performance. Roy et al. [10] analyzed an ORC using working fluid such as R-12, R-123 and R-134a. The results were compared with respect to their abilities to convert low-grade heat source energy to power. The results show that R-123 has the maximum work output and efficiencies among all the selected fluids. Shengjun et al. [11] presented an investigation on the parameter optimization and performance comparison of the fluids in subcritical ORC and transcritical power cycle in low-temperature binary geothermal power system. The optimization procedure was conducted with a simulation program written in Matlab using five indicators: thermal efficiency, exergy efficiency, recovery efficiency, heat exchanger area per unit power output and the levelized energy cost. With the given heat source and heat sink conditions, performances of the working fluids were evaluated and compared under their optimized internal operation parameters. The optimum cycle design and the corresponding operation parameters were provided simultaneously.

Yamada et al. [12] investigated thermal efficiency of low-to medium-temperature ORCs using HFO-1234yf. The efficiency of HFO-1234yf was compared with that of other working fluids. Fernandez et al. [13] carried out thermodynamic analysis of high-temperature regenerative ORCs using siloxanes as working fluids. The analysis includes saturated and superheated, subcritical and supercritical cycles with linear and cyclic siloxanes. Simple linear siloxanes in saturated regenerative schemes show good efficiencies and ensure thermal stability of the working fluid. Li et al. [14] carried out thermodynamic analysis of ORC with ejector. The experiments and theoretical analyses were carried out in the same operation conditions. A Double ORC was also introduced in order to analyze and compare the ORC with ejector with the ORC. The thermal performance of Double ORC was superior to ORC with ejector.

In addition, artificial intelligence methods have also been applied to ORC in recent years. Rashidi et al. [15] carried out parametric analysis and optimization of regenerative Clausius and ORCs with two feedwater heaters. Artificial bee colony and artificial neural network methods for the parametric optimization were used. R717 and water as working fluid were used. Finally it is found that the maximum values of the specific network, the thermal efficiency and the exergy efficiency for R717 are greater than those for water. Wang et al. [16] carried out parametric optimization design for supercritical CO_2 power cycle using genetic algorithm and artificial neural network. It is shown that the key thermodynamic parameters, such as turbine inlet pressure, turbine inlet temperature and environment temperature have significant effects on the performance of the supercritical CO_2 power cycle and exergy destruction in each component. It is also shown that the optimum thermodynamic parameters of supercritical CO_2 power cycle can be predicted with good accuracy using artificial neural network under variable waste heat conditions. Wang et al. [17] presented thermodynamic analysis and optimization of an ORC using low grade heat source. Parametric optimization is conducted to maximize the ratio of net power output to total heat transfer area considering economic factor by Genetic Algorithm. By parametric optimization, the ORC system with isobutane has the best system performance than that with R123 or R245fa. Arslan and Yetik [18] optimized supercritical ORC-Binary using artificial neural network. In the study, the trained algorithms also showed that the predicted values could be used to design an ORC-Binary power plant with less data and a high level of accuracy.

As can be seen from the literature review presented above, studies on use of artificial intelligence methods to energy systems and different ORC systems are available. However, studies on efficiency analysis of ORC with internal heat exchanger by using ANN are not available in the literature. In addition, studies on efficiency analysis of the ORC with internal heat exchanger using refrigerants R410a and R407c are very limited. In this study, in order to determine thermal efficiency of ORC with internal heat exchanger using refrigerants R410a and R407c artificial neural network (ANN) model was used. The results obtained from ANN model were compared with actual

results. The thermal efficiency of ORC with internal heat exchanger with these models was estimated successfully. In addition, new formulations obtained from ANN are presented for the calculation of the thermal efficiency values. The use of this new formulation, which can be employed with any programming language or spreadsheet program for estimation of the thermal efficiency of IHEORC, as described in this paper, may make the use of dedicated ANN or Solkane software unnecessary. The results of this study will help to obtain a very accurate and fast forecast of the thermal efficiency of ORC with internal heat exchanger.

2 Calculation of thermal efficiency

Fundamental equations are introduced that are based on the energy balance of the ORC with internal heat exchanger according to the first law of thermodynamics. The analysis ignores the pressure loss from heat exchangers and piping. And each component is considered as a steady-state steady-flow system. Further details of the mathematical model are given as follows:

Pump: The work required in the pump is given by:

$$W_P = \dot{m}(h_2 - h_1) \tag{1}$$

Evaporator: The heat transfer rate into the working fluid through the evaporator is defined as:

$$Q_E = \dot{m}(h_4 - h_3) \tag{2}$$

Turbine: The work produced in the turbine is given by:

$$W_T = \dot{m}(h_4 - h_5) \tag{3}$$

Condenser: The heat transfer rate in the condenser is given by:

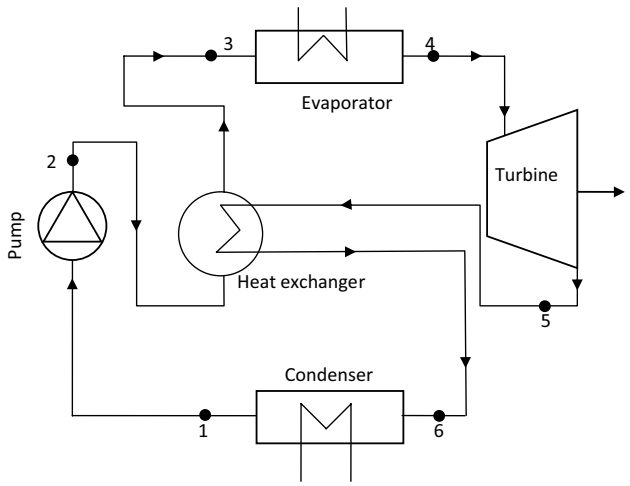

Fig. 1 Organic Rankine cycle with internal heat exchanger

$$Q_C = \dot{m}(h_6 - h_1) \tag{4}$$

The thermal efficiency of the ORC with internal heat exchanger is related to input power, output power and heat transfer rate. The thermal efficiency of the cycle is defined as:

$$\eta = \frac{W_T - W_P}{Q_E} = \frac{(h_4 - h_5) - (h_2 - h_1)}{(h_4 - h_3)} \tag{5}$$

Here, h is the enthalpy, $\dot{m}$ is the mass flow rate of the working fluid, the subscript numbers, 1–6, represent the state of the working fluid corresponding to the state numbers shown in Fig. 1.

3 Model development

In this study, the thermal efficiency of ORC with internal heat exchanger depending on the evaporator temperature (T_E), condenser temperature (T_C), superheating temperature (T_{SH}) and subcooling temperature (T_{SC}) for R410a and R407c is predicted using ANN approach. In Table 1, the input- output parameters used in the analysis are shown.

The performance of ANN model for training and testing data sets were evaluated according to statistical criteria such as, the Root-Mean-Squared Error (RMSE), the coefficient of determination (R^2) and the coefficient of variation (cov). These statistical criteria's will be used to compare the predicted and actual values. During learning the error is estimated by RMSE defined as [19]:

$$RMSE = \sqrt{\frac{\sum_{m=1}^{n} (y_{p,m} - t_{m,m})^2}{n}} \tag{6}$$

In addition, the coefficient of determination (R^2) and coefficient of variation (cov) in percent are defined as follows [19]:

$$R^2 = 1 - \frac{\sum_{m=1}^{n} (t_{m,m} - y_{p,m})^2}{\sum_{m=1}^{n} (t_{m,m} - \bar{t}_{m,m})^2} \tag{7}$$

$$\text{cov} = \frac{RMSE}{|\bar{t}_{m,m}|} 100 \tag{8}$$

Table 1 Input and output parameters

Working fluid	Input parameters	Output parameters
R410a	Evaporator temperature (T_E)	Thermal efficiency (η)
	Condenser temperature (T_C)	
R407c	Superheating temperature (T_{SH})	
	Subcooling temperature (T_{SC})	

where n is the number of data patterns, $y_{p,m}$ indicates the predicted, $t_{m,m}$ is the measured value of one data point m, and $\bar{t}_{m,m}$ is the mean value of all measure data points.

In order to achieve the optimal result, different algorithms and different numbers of hidden neurons were used. The computer program was performed under MATLAB environment using the neural network toolbox. The back propagation learning algorithm has been used in a feed forward, single hidden layer neural network. The variants of the algorithm used in the study are the Levenberg–Marquardt (LM) and Scaled Conjugate Gradient (SCG) algorithms. The actual input data of the various parameters need to be normalized in the range (0–1). For this purpose the actual values of each parameter are divided with the coefficients shown in Table 2.

A log-sigmoid activation function was used for the hidden and output layer. The activation function used is given by:

$$F(z) = \frac{1}{1 + e^{-z}} \tag{9}$$

where z is the weighted sum of the input.

The next step in the development of the ANN model was the determination of the optimum number of neurons in the hidden layer. This was identified using a trial and error procedure by varying the number of hidden neurons from 3 to 12. The data set for the thermal efficiency of ORC with internal heat exchanger available included 153 data patterns. From these, 101 data patterns were used for training the network, and 26 data patterns were randomly selected and used as the test data set. 26 data patterns were used for validation. The data set for testing and validation were taken from Solkane Software. Solkane is a software package for calculating the thermophysical and thermodynamic properties of fluids. In addition, Solkane software performs calculations of cycles as some refrigeration and ORC cycle [20].

Table 2 Normalization coefficients for input and output parameters

Refrigerant	Input parameter	Coefficient
R410a	Evaporator temperature (T_E)	68
	Condenser temperature (T_C)	42
	Superheating temperature (T_{SH})	22
	Subcooling temperature (T_{SC})	27
R407c	Evaporator temperature (T_E)	84
	Condenser temperature (T_C)	27
	Superheating temperature (T_{SH})	22
	Subcooling temperature (T_{SC})	22

The actual values are divided with the above coefficients to obtain the normalized values

Table 3 Statistical values of thermal efficiency for R410a working fluid

Algorithm	RMSE	Cov	R^2
LM-3	0.0219298	0.263970128	0.99732
LM-4	0.0176864	0.212892195	0.998257
LM-5	0.0174786	0.210389994	0.998298
LM-6	0.0186466	0.224449389	0.998062
LM-7	0.0201153	0.242129179	0.997745
LM-8	0.0174519	0.210069269	0.998303
LM-9	0.0179397	0.215940625	0.998207
LM-10	0.0172904	0.208124845	0.998334
LM-11	0.0174124	0.209594033	0.99831
LM-12	0.0184362	0.221917762	0.998106
SCG-3	0.0182846	0.220091846	0.998137
SCG-4	0.0338367	0.407293391	0.99362
SCG-5	0.0110604	0.133134674	0.999318
SCG-6	0.0131051	0.157746645	0.999043
SCG-7	**0.0098417**	**0.118464407**	**0.99946**
SCG-8	0.0149269	0.179675049	0.998758
SCG-9	0.0131764	0.158604486	0.999032
SCG-10	0.0152644	0.183738246	0.998702
SCG-11	0.012245	0.147393582	0.999164
SCG-12	0.0123128	0.148210122	0.999155

Bold values indicate statistical values of the most optimal topology for thermal efficiency prediction

Table 4 Statistical values of thermal efficiency for R407c working fluid

Algorithm	RMSE	Cov	R^2
LM-3	0.015148	0.146961	0.999169
LM-4	0.014069	0.136493	0.999283
LM-5	0.014989	0.145417	0.999187
LM-6	0.014846	0.144029	0.999202
LM-7	0.014402	0.139719	0.999249
LM-8	0.014039	0.136196	0.999287
LM-9	0.014659	0.142215	0.999222
LM-10	0.015003	0.145554	0.999185
LM-11	0.014652	0.142147	0.999223
LM-12	0.014371	0.139423	0.999252
SCG-3	0.00582	0.00582	0.999877
SCG-4	0.004007	0.038878	0.999942
SCG-5	**0.003984**	**0.038655**	**0.999943**
SCG-6	0.008359	0.081097	0.999747
SCG-7	0.006422	0.062302	0.999851
SCG-8	0.004073	0.039511	0.99994
SCG-9	0.005129	0.049757	0.999905
SCG-10	0.009892	0.095967	0.999646
SCG-11	0.005197	0.05042	0.999902
SCG-12	0.005489	0.053253	0.999891

Bold values indicate statistical values of the most optimal topology for thermal efficiency prediction

Statistical values such as RMSE, R^2 and cov are given in Table 3 for the R410a working fluid and in Table 4 for the R407c working fluid.

From the data presented in Table 3 for the R410a working fluid, the SCG algorithm with seven neurons in the hidden layer (SCG-7) appeared to be the most optimal topology. The R^2-value for the thermal efficiency values of the system working with R410a is 0.99946 which can be considered as very satisfactory. Figure 2 shows the architecture of the ANN used in the thermal efficiency prediction for the R410a working fluid. The decrease of the mean square error (MSE) during the training process of this topology is shown in Fig. 3. The regression curve of the output variable (thermal efficiency) for the test data set is shown in Fig. 4. The correlation coefficient obtained in this case is 0.9326, which is very satisfactory.

From the data presented in Table 4 for the R407c working fluid, the SCG algorithm with five neurons in the hidden layer (SCG-5) appeared to be the most optimal topology. The R^2-value for the thermal efficiency values of the

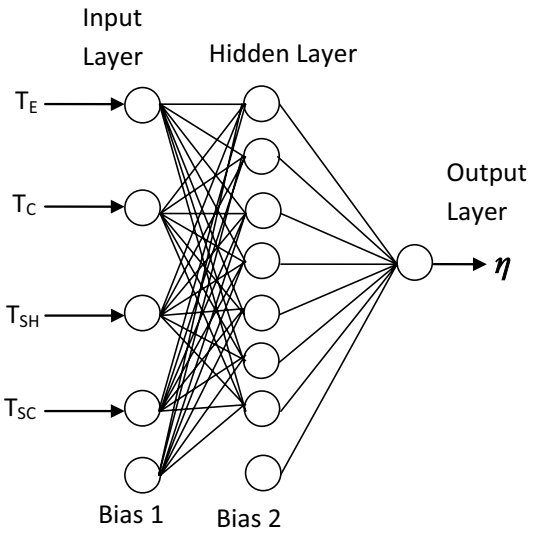

Fig. 2 Architecture of the ANN used in the thermal efficiency prediction for the R410a working fluid

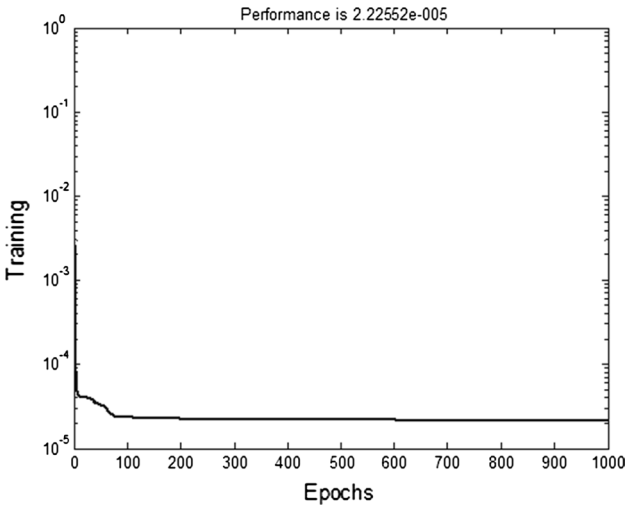

Fig. 3 Variation of mean square error with training epochs for the thermal efficiency (for the R410a)

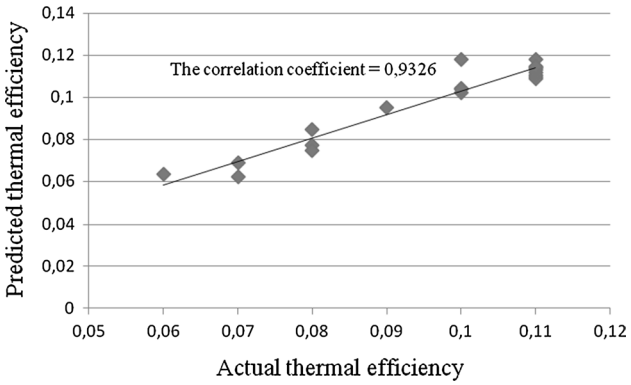

Fig. 4 Comparison of actual and ANN predicted values of the thermal efficiency for the test data set (for the R410a)

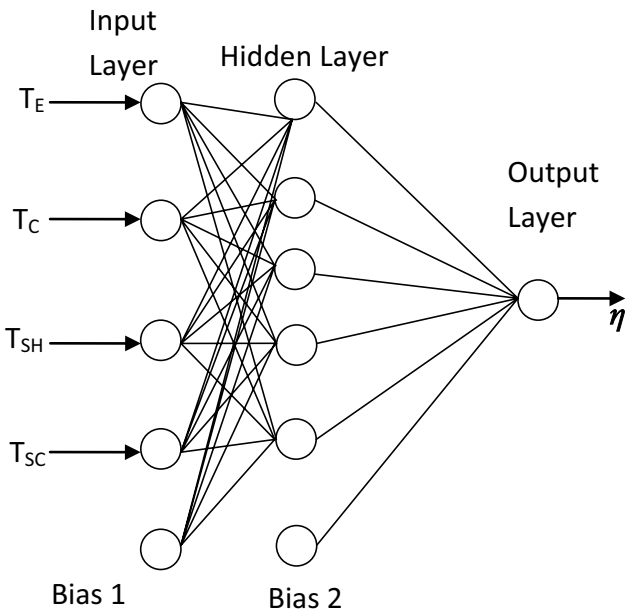

Fig. 5 Architecture of the ANN used in the thermal efficiency prediction for the R407c working fluid

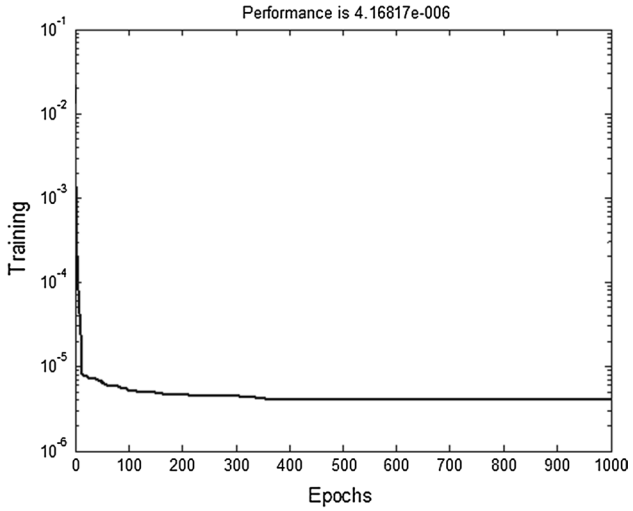

Fig. 6 Variation of mean square error with training epochs for the thermal efficiency (for the R407c)

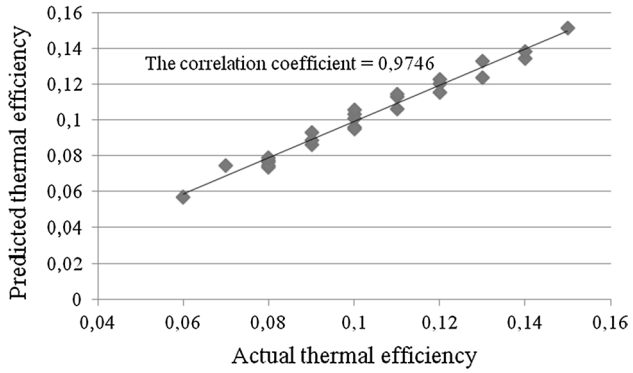

Fig. 7 Comparison of actual and ANN predicted values of the thermal efficiency for the test data set (for the R407c)

system working with R407c is 0.999943 which can be considered as very satisfactory. Figure 5 shows the architecture of the ANN used in the thermal efficiency prediction for the R407c working fluid. The decrease of the mean square error (MSE) during the training process of this topology is shown in Fig. 6. The regression curve of the output variable (thermal efficiency) for the test data set is shown in Fig. 7. The correlation coefficient obtained in this case is 0.9746, which is very satisfactory.

4 Results and discussion

The mathematical formulations derived from the ANN model are presented here. In order to determine the thermal efficiency of ORC with internal heat exchanger, the following equations are used derived from the ANN methodology:

$$E_i = \sum_{n=1}^{4} I_n w_{ni} + b_n \tag{10}$$

$$F_i = \frac{1}{1 + e^{-E_i}} \tag{11}$$

In the above equations for E_i the first two values are the multiplication of the input parameters (I_n) with their weights at location n and the last constant value (b_n) represent the bias term. The subscript i represent the number of hidden neuron. The four input parameters are:

I_1 = Evaporator temperature (T_E)
I_2 = Condenser temperature (T_C)
I_3 = Superheating temperature (T_{SH})
I_4 = Subcooling temperature (T_{SC})

For the thermal efficiency estimation of R410a working fluid, the best approach, which has minimum errors, is obtained from a network with 7 hidden neurons. Thus 7 pairs of equations, i.e., E_1 to E_7 and F_1 to F_7 are required, which represent the summation and activation functions of each neuron of the hidden layer respectively. The coefficients of Eq. (10) are given in Table 5.

For the thermal efficiency estimation of R407c working fluid, the best approach, which has minimum errors, is obtained from a network with 5 hidden neurons. Thus 5 pairs of equations, i.e., E_1 to E_5 and F_1 to F_5 are required, which represent the summation and activation functions of each neuron of the hidden layer respectively. The coefficients of Eq. (10) are given in Table 6.

Finally, the thermal efficiency values depending on the evaporator temperature (T_E), condenser temperature (T_C), superheating temperature (T_{SH}) and subcooling temperature (T_{SC}) for R410a can be computed from:

$$\begin{aligned} E_8 = {} & F_1^*(132.2658) + F_2^*(-156.9813) + F_3^*(0.2007) \\ & + F_4^*(19.5787) + F_5^*(123.5142) + F_6^*(53.5699) \\ & + F_7^*(-19.2948) - 31.2036 \end{aligned} \tag{12}$$

$$\eta = \left(\frac{1}{1 + e^{-E_8}} \right) \tag{13}$$

Similarly, the thermal efficiency values depending on the same input parameters for R407c can be computed from:

$$\begin{aligned} E_6 = {} & F_1^*(-47.5858) + F_2^*(36.1811) + F_3^*(0.57398) \\ & + F_4^*(14.6332) + F_5^*(-16.5511) + 9.6051 \end{aligned} \tag{14}$$

$$\eta = \left(\frac{1}{1 + e^{-E_6}} \right) \tag{15}$$

Table 5 Weight coefficients and bias values of the ANN used for the thermal efficiency estimation of R410a

Neuron position (w_{ni})	I_1 (T_E)	I_2 (T_C)	I_3 (T_{SH})	I_4 (T_{SC})	b_n
1	−48.8949	−16.1567	−87.5298	52.8859	82.2649
2	3.9666	−6.7727	−10.6998	23.7587	3.9009
3	176.8773	−26.0785	−533.9288	85.7691	17.4549
4	5.8289	31.0526	−33.5122	13.0564	−8.132
5	−4.8019	15.3242	259.5231	−153.8313	−72.7063
6	4.6672	−3.788	−0.55058	0.99202	2.9034
7	5.9778	36.5705	−37.0765	14.9577	−9.5938

Table 6 Weight coefficients and bias values of the ANN used for the thermal efficiency estimation of R407c

Neuron position (w_{ni})	I_1 (T_E)	I_2 (T_C)	I_3 (T_{SH})	I_4 (T_{SC})	b_n
1	−0.32715	1.9768	1.2053	−7.8577	8.9065
2	−0.68204	1.3867	0.74629	−7.9844	9.4548
3	6.98	−7.6312	7.0907	12.3607	−15.9515
4	−9.0445	3.5869	−1.1868	2.0313	1.6546
5	−8.6169	3.3849	−1.0875	1.8111	1.6066

Table 7 Comparison of actual and ANN estimated thermal efficiency values of organic Rankine cycle with internal heat exchanger for R410a

T_E (°C)	T_C (°C)	T_{SH} (°C)	T_{SC} (°C)	Actual thermal efficiency	ANN predicted thermal efficiency	Error	Percentage difference (%)[a]
40	15	5	5	0.07	0.066798468	0.003202	4.573617
49	15	5	5	0.09	0.091754541	−0.00175	−1.94949
52	15	5	5	0.1	0.097772315	0.002228	2.227685
40	20	8	6	0.06	0.0628524	−0.00285	−4754
61	20	8	6	0.1	0.100485691	−0.00049	−0.48569
45	25	10	10	0.06	0.06054036	−0.00054	−0.9006
55	25	10	10	0.08	0.080825063	−0.00083	−1.03133
60	25	10	10	0.09	0.086704767	0.003295	3.66137
62	15	10	25	0.1	0.104012145	−0.00401	−4.01214
42	8	7	22	0.08	0.084688885	−0.00469	−5.86111
43	8	7	22	0.09	0.08525164	0.004748	5.275956
44	8	7	22	0.09	0.085963271	0.004037	4.485255
55	8	7	22	0.11	0.10430265	0.005697	5.179409
56	8	7	22	0.11	0.105910079	0.00409	3.71811
57	8	7	22	0.11	0.107305934	0.002694	2.449151

[a] Percentage difference (%) = (error/actual thermal efficiency) × 100

Tables 7 and 8 give a comparison of the actual thermal efficiency values with the results of ANN model for the ORC with internal heat exchanger for R410a and R407c respectively.

Figures 8 and 9 give a comparison of the actual thermal efficiency values with the results of ANN model for the ORC with internal heat exchanger in the different evaporator temperatures for the R410a and R407c respectively. As can be seen in Figs. 8 and 9, the actual thermal efficiency values for both working fluids agree with the results of ANN model.

5 Conclusion

The thermal efficiency values of an ORC with internal heat exchanger was estimated depending on the evaporator temperature, condenser temperature, superheating temperature

Table 8 Comparison of actual and ANN estimated thermal efficiency values of organic Rankine cycle with internal heat exchanger for R407c

T_E (°C)	T_C (°C)	T_{SH} (°C)	T_{SC} (°C)	Actual thermal efficiency	ANN predicted thermal efficiency	Error	Percentage difference (%)[a]
44	15	5	5	0.08	0.0793027	0.000697	0.871624
54	15	5	5	0.1	0.10043243	−0.00043	−0.43243
78	15	5	10	0.13	0.13407813	−0.00408	−3.13702
80	15	5	10	0.14	0.13549913	0.004501	3.21491
41	20	5	15	0.06	0.06098534	−0.00099	−1.64223
70	15	15	20	0.14	0.13628604	0.003714	2.652828
60	20	5	15	0.1	0.09732584	0.002674	2.674157
67	20	5	15	0.11	0.10733336	0.002667	2.42422
81	20	5	15	0.12	0.12210949	−0.00211	−1.75791
50	25	18	5	0.08	0.07821402	0.001786	2.232473
52	25	18	5	0.08	0.08257185	−0.00257	−3.21482
55	25	18	5	0.09	0.08883853	0.001161	1.290526
56	25	18	5	0.09	0.0907729	−0.00077	−0.85878
62	25	18	5	0.1	0.10015197	−0.00015	−0.15197
63	25	18	5	0.1	0.10135288	−0.00135	−1.35288

[a] Percentage difference (%) = (error/actual thermal efficiency) × 100

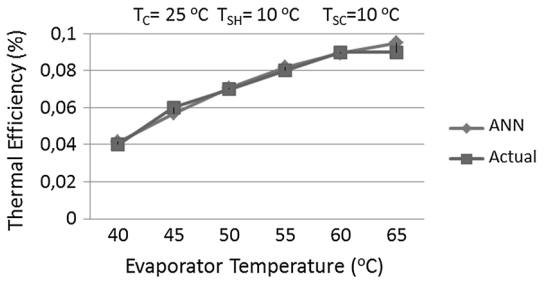

Fig. 8 Comparison between actual and ANN thermal efficiency for R410a

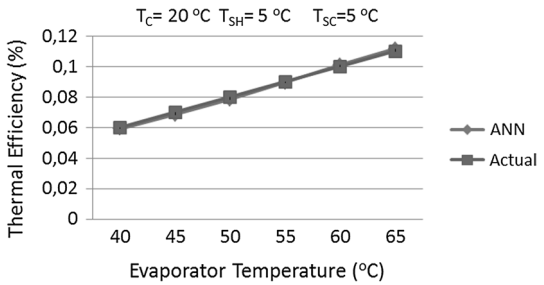

Fig. 9 Comparison between actual and ANN thermal efficiency for R407c

and subcooling temperature values by using ANN. The ANN is successfully applied to determine the thermal efficiency values of the system working with R410a and R407c. The R^2-value for the thermal efficiency values of a system working with R410a is 0.99946 and the R^2-value for the thermal efficiency values of a system working with R407c is 0.999943 which can be considered as very satisfactory. In order to calculate the thermal efficiency values, mathematical formulations were derived from the ANN model. The use of this new formulation, which can be employed with any programming language or spreadsheet program for estimation of the thermal efficiency of IHEORC, as described in this paper, may make the use of dedicated ANN or Solkane software unnecessary. This method will help engineers to obtain a very accurate and fast forecast of the thermal efficiency of ORC with internal heat exchanger.

References

1. Tchanche BF, Lambrinos G, Frangoudakis A, Papadakis G (2011) Low-grade heat conversion into power using organic rankine cycles—a review of various applications. Renew Sustain Energy Rev 15:3963–3979
2. Algieri A, Morrone P (2012) Comparative energetic analysis of high-temperature subcritical and transcritical organic Rankine cycle (ORC). A biomass application in the Sibari district. Appl Therm Eng 36:236–244
3. Chen Q, Xu J, Chen H (2012) A new design method for organic Rankine cycles with constraint of inlet and outlet heat carrier fluid temperatures coupling with the heat source. Appl Energy 98:562–573
4. Delgado-Torres AM, Garcia-Rodriguez L (2010) Analysis and optimization of the low-temperature solar organic Rankine cycle (ORC). Energy Convers Manag 51:2846–2856
5. Kuo CR, Hsu SW, Chang KH, Wang CC (2011) Analysis of a 50 kW organic Rankine cycle system. Energy 36:5877–5885
6. Kang SH (2012) Design and experimental study of ORC (organic Rankine cycle) and radial turbine using R245fa working fluid. Energy 41:514–524

7. Aljundi IH (2011) Effect of dry hydrocarbons and critical point temperature on the efficiencies of organic Rankine cycle. Renewable Energy 36:1196–1202
8. Wang ZQ, Zhou NJ, Guo J, Wang XY (2012) Fluid selection and parametric optimization of organic Rankine cycle using low temperature waste heat. Energy 40:107–115
9. Sun J, Li W (2011) Operation optimization of an organic rankine cycle (ORC) heat recovery power plant. Appl Therm Eng 31:2032–2041
10. Roy JP, Mishra MK, Misra A (2010) Parametric optimization and performance analysis of a waste heat recovery system using organic Rankine cycle. Energy 35:5049–5062
11. Shengjun Z, Huaixin W, Tao G (2011) Performance comparison and parametric optimization of subcritical organic Rankine cycle (ORC) and transcritical power cycle system for low-temperature geothermal power generation. Appl Energy 88:2740–2754
12. Yamada N, Mohamad MNA, Kien TT (2012) Study on thermal efficiency of low- to medium-temperature organic Rankine cycles using HFO-1234yf. Renewable Energy 41:368–375
13. Fernandez FJ, Prieto MM, Suarez I (2011) Thermodynamic analysis of high-temperature regenerative organic Rankine cycles using siloxanes as working fluids. Energy 36:5239–5249
14. Li X, Zhao C, Hu X (2012) Thermodynamic analysis of organic Rankine cycle with ejector. Energy 42:342–349
15. Rashidi MM, Galanis N, Nazari F, Basiri Parsa A, Shamekhi L (2011) Parametric analysis and optimization of regenerative Clausius and organic Rankine cycles with two feedwater heaters using artificial bees colony and artificial neural network. Energy 36:5728–5740
16. Wang J, Sun Z, Dai Y, Ma S (2010) Parametric optimization design for supercritical CO_2 power cycle using genetic algorithm and artificial neural network. Appl Energy 87:1317–1324
17. Wang J, Yan Z, Wang M, Ma S, Dai Y (2013) Thermodynamic analysis and optimization of an (organic Rankine cycle) ORC using low grade heat source. Energy 49:356–365
18. Arslan O, Yetik O (2011) ANN based optimization of supercritical ORC-Binary geothermal power plant: simav case study. Appl Therm Eng 31:3922–3928
19. Bechtler H, Browne MW, Bansal PK, Kecman V (2001) New approach to dynamic modeling of vapor-compression liquid chillers: artificial neural Networks. Appl Therm Eng 21:941–953
20. Solkane Software. http://www.solvay-fluor.com/docroot/fluor/static_files/attachments/download.htm [27.12.09]